Int J Adv Manuf Technol (2015) 76:1403–1410
DOI 10.1007/s00170-014-6364-8

ORIGINAL ARTICLE

Friction stir blind riveting of carbon fiber-reinforced polymer composite and aluminum alloy sheets

Junying Min · Yongqiang Li · Jingjing Li · Blair E. Carlson · Jianping Lin

Received: 2 June 2014 / Accepted: 8 September 2014 / Published online: 18 September 2014

Abstract A friction stir blind riveting (FSBR) process is used to fabricate joints of carbon fiber-reinforced polymer composite (CFRP) and aluminum alloy AA6111 sheets in a lap shear configuration. Given the 9,000 rpm spindle speed upper limit of conventional computer numerically controlled machines, the maximum feed rate for FSBR joining CFRP to itself is found to be 120 mm min^{-1} above which quality issues such as cracking of the CFRP sheet predominate. However, the maximum feed rate during dissimilar joining of CFRP to AA6111 can be 420 mm min^{-1} when the CFRP top sheet is supported by the AA6111 bottom sheet. The maximum lap shear tensile load of the joints shows little dependence on the spindle speed and feed rate during FSBR. The different stack-up sequences of the CFRP and AA6111 lead to different maximum loads, displacements to fracture, and locations of fracture initiation, i.e., in the CFRP vs. in the AA6111.

Keywords Friction stir blind riveting · Al alloy · Carbon fiber-reinforced polymer · Joining

1 Introduction

Carbon fiber-reinforced polymer (CFRP) composites have been increasingly applied in the automotive sector as a mass savings and performance-enhancing alternative to metals (e.g., crashworthiness, noise, vibration, and fatigue resistance). However, due to the high cost of CFRP, cars and trucks are likely to be composed of a mix of metals and CFRP. Therefore, mixed material joining of CFRP composites and metals will be a key enabling technology for wider adoption of lightweight CFRP in automotive applications.

Mechanical fastening/joining (e.g., by rivets [1]), adhesive bonding [2], laser welding [3], gas metal arc welding [4], etc. have been applied to join composites and metals. For example, Hufenbach et al. [5] experimentally studied and numerically simulated the lap shear tensile performance of riveted CFRP and Al alloy joints. Two CFRP sheets were adhesively bonded by Casas-Rodriguez et al. [6] and the impact-fatigue performance investigated. Anyfantis and Tsouvalis [7] fabricated joints of CFRP and mild steels by adhesive bonding. They found that an increase (200 %) of overlap length resulted in an increase (100 %) to the joints' lap shear strength. The laser welding method was recently developed to join composites and metals, e.g., CFRP and steel were joined using a continuous wave diode laser by Jung et al. [8, 9]. They found that the CFRP and steel workpieces were tightly bonded at an atomic or molecular level. All three types of joining methods have their merits and shortcomings. Although holes must be predrilled in parts for conventional mechanical fastening and alignment of the holes in parts prior to fastening is not trivial in a manufacturing setting, mechanical fastening is relatively easy and efficient in joining dissimilar materials. Adhesive bonding distributes the load along a continuous joint line, but structural adhesive bonding [10] often requires heated curing and the temperature may cause distortion or even damage to CFRP parts. Formulation of adhesives that bond CFRP on one side and metal on the other side is also challenging. Laser welding of CFRP and metals can also produce a continuous weld line for load distribution, but the beam application must be limited to the metal side and to thermoplastic CFRP materials only [9].

J. Min · J. Li
Department of Mechanical Engineering, University of Hawaii at Manoa, 2540 Dole Street, Honolulu, HI 96822, USA

Y. Li · B. E. Carlson
General Motors Research & Development, 30500 Mound Road, Warren, MI 48090, USA

J. Lin (✉)
School of Mechanical Engineering, Tongji University, 1239 Siping Road, 200092 Shanghai, China
e-mail: jplin58@tongji.edu.cn

Recently, a friction stir blind riveting (FSBR) process was developed to join sheet metals [11, 12]. In FSBR (illustrated in Fig. 1), a blind rivet rotating at a high spindle speed, which can be between 1,000 and 20,000 rpm, penetrates the workpieces without predrilled holes under a normal force. Due to the frictional heat generated between the rivet tip and the workpieces, the normal force required to penetrate the heated and softened workpieces is substantially lower than when the rivet was pressed through cold metals. When the rivet cap reaches the top surface of the upper workpiece, the motion of the rivet is stopped and the mandrel is pulled and broken at a weakened notch located near the top of the rivet cap. At the same time, the shank is expanded, and a rivet tail, which locks the workpieces tightly, is formed.

In this work, FSBR was used to join CFRP and aluminum alloy sheets. Three combinations of material stack-ups in a lap shear joint configuration were fabricated: CFRP-CFRP, CFRP-AA6111, and AA6111-CFRP (the first material denotes the upper sheet as shown in Fig. 1). The effects of spindle speed (ω) and feed rate (v) on the force and torque during frictional penetration and the tensile load of the FSBR joints have been analyzed and discussed.

2 Experimental details

2.1 Materials

The materials used in this work were injection-molded carbon fiber-reinforced thermoplastic sheets and hot rolled AA6111 aluminum alloy sheets with thicknesses of 3.0 and 0.9 mm, respectively. CFRP plaques with dimensions of 102 mm wide, 203 mm long, and 3.0 mm thick were molded at 320 °C using pellets of BASF Ultramid® T KR 4370 C6 PA6/6T-CF30 with 30 wt% random short carbon fiber. The plaques were waterjet cut into 127 mm long and 38 mm wide rectangular workpieces, where the length was parallel to the molding material flow direction. Hot rolled AA6111 sheets were sheared into rectangular shapes (also 127 mm long and 38 mm wide) with the width direction aligned with the rolling direction. The nominal mechanical and physical properties provided by suppliers of both CFRP and AA6111 sheets are listed in Table 1. The blind rivets used in this work were Monobolt® SSPV-06-04 mild steel rivets with a shank diameter of 4.8 mm provided by Avdel.

2.2 Friction stir blind riveting method

Lap shear joints from three material combinations were fabricated by the FSBR process, namely, CFRP-CFRP (combination I), AA6111-CFRP (combination II), and CFRP-AA6111 (combination III). The fixture used for clamping the workpieces during fabrication of the FSBR joints is shown in Fig. 2. This was installed on the top of a dynamometer (Kistler Type 9273). The workpieces and spacers were fixed with two clamping platens as illustrated in Fig. 2a. The force and torque data measured with the dynamometer during FSBR were acquired with a National Instruments data acquisition system at 100 points per second. The range of the force sensor was 5 kN with a resolution of 0.01 kN, and the range of the torque sensor was 100 Nm with a resolution of 0.1 Nm.

The FSBR joints were fabricated using a Makino CNC machine using three spindle speeds: 3,000, 6,000, and 9,000 rpm. At each spindle speed, five feed rates 60, 120, 240, 420, and 600 mm min^{-1} were evaluated. When the rivet penetrated through both workpieces and the shank head was in

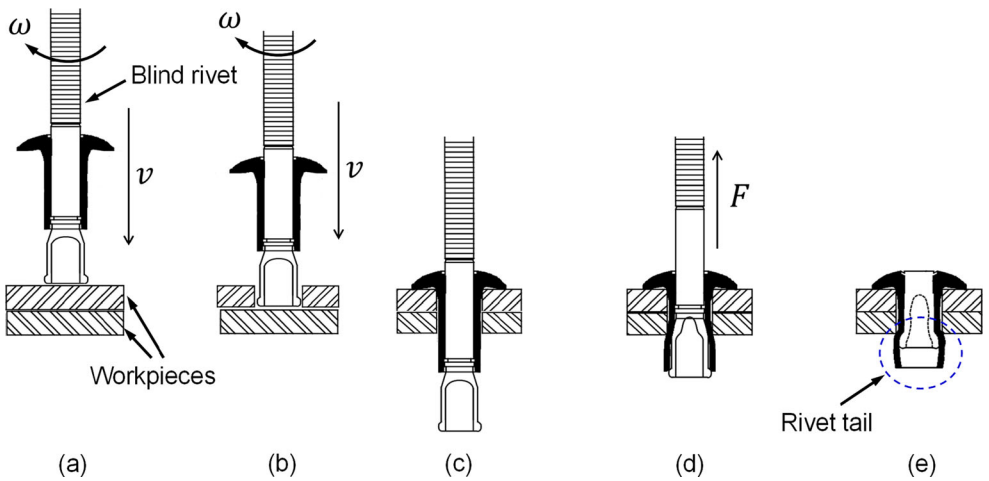

Fig. 1 Illustration of the friction stir blind riveting (FSBR) process. **a** The rotating blind rivet approaches the workpieces with feed rate (v) and high spindle speed (ω); **b** the rotating blind rivet penetrates the frictionally heated and softened top workpiece; **c** the blind rivet has penetrated both workpieces, and the shank head is in contact with the top workpiece; **d** the mandrel of the blind rivet is pulled with a force (F); **e** the mandrel is broken and an FSBR joint is obtained. **d**, **e** Together are also known as the tail forming process [13]

Table 1 Mechanical and physical properties of the CFRP and Al alloy used in this work at room temperature

Material	Tensile strength [MPa]	Yield strength [MPa]	Tensile modulus [GPa]	Strain at break [%]	Glass transition temperature [°C]	Melting temperature [°C]
CFRP	250	–	23	2	105 (amorphous phase)	295 (crystalline phase)
AA6111	307	178	70	25	–	635

contact with the upper workpiece, the mandrel was unloaded from the spindle of the CNC machine and the workpieces were unclamped from the fixture. The mandrel was pulled with a handheld rivet gun to lock the workpieces and break the mandrel to finish the whole FSBR process. This multistep operation was undertaken in a laboratory setting, as the CNC machine was not designed to pull the rivet. In a real manufacturing process, the whole operation is expected to be conducted with a single equipment that incorporates all functions: rotation and driving of the mandrel through the workpieces under programmed speeds, sitting the mandrel head on the upper workpiece, pulling the rivet to lock the workpieces, and disposing of the severed portion of the mandrel.

2.3 Tensile tests

Lap shear joints were tensile tested with a universal Instron 5582 testing machine at a crosshead speed of 5 mm min^{-1} and room temperature. Two spacers were used in the tensile tests to keep the joint parallel to the tensile axis. The gripping area on both ends was 38 mm×38 mm^2.

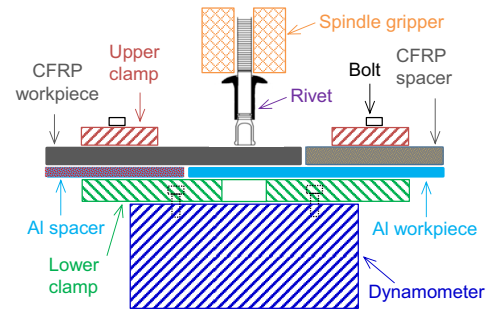

(a)

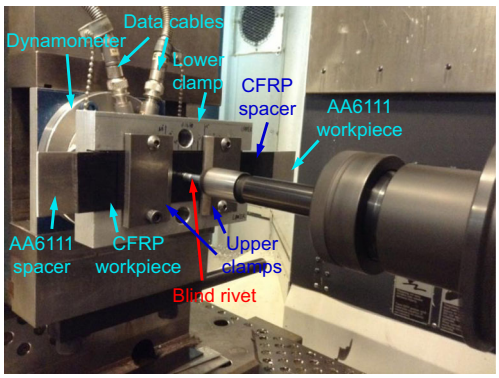

(b)

Fig. 2 **a** Illustration for the experimental setup and (**b**) the actual experimental setup used in the FSBR tests

3 Process windows

A previous study [13] on the FSBR process using 0.9 mm thick AA6111 alloy sheets reported that the AA6111-AA6111 joints have a wide process window 120 mm $min^{-1} \leq v \leq$ 780 mm min^{-1} and 3,000 rpm$\leq\omega\leq$9,000 rpm using the same rivet as this work without any quality issue. It is noted that the upper limits of the feed rate and the rotational speed were not related to the joint quality but rather to the practical limits of the Makino CNC machine. The process windows for joining CFRP and AA6111 alloy sheets are reported below.

Table 2 shows the process window of the CFRP-CFRP joints (combination I). It shows that the two 3 mm thick CFRP workpieces could only be joined at relatively high spindle speeds and low feed rates. Lower spindle speeds or higher feed rates created quality issues such as brittle spalling near the bottom of the sheet because of excessive normal forces, as illustrated in Fig. 3a. This situation is considered as a quality issue rather than a bad joint since the parts could still be locked with the rivet and substantial mechanical integrity preserved. However, the quality issue generally lowers the tensile strength of the FSBR joints, which still depends on the fracture mode of the joints when subjected to lap shear tension. The details are described in Section 5. The quality issue was also observed when joining CFRP and AA6111, in which case the brittle spalling occurred on the CFRP bottom surface in contact with the AA6111. Figure 3b shows a semifinished, i.e., interrupted CFRP-AA6111 joint (the joining process was

Table 2 Process window of the CFRP-CFRP joints by FSBR

Spindle speed [rpm]	Feed rate [mm min^{-1}]				
	60	120	270	420	600
3,000	QI	QI	–	–	–
6,000	√	QI	QI	–	–
9,000	√	√	QI	QI	–

√ sound joint, *QI* quality issue, – not tested

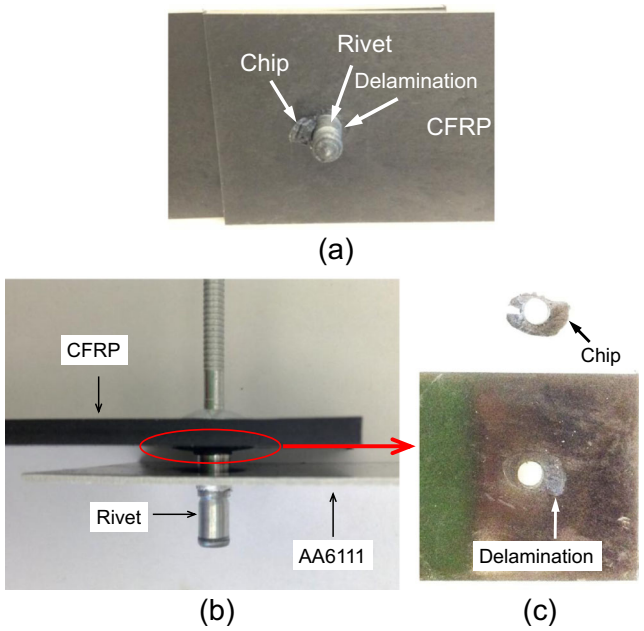

Fig. 3 **a** An interrupted CFRP-CFRP FSBR joint (ω=6,000 rpm and v=120 mm min^{-1}) and **b** an interrupted CFRP-AA6111 FSBR joint (ω=6,000 rpm and v=600 mm min^{-1}) with quality issue, where a chip delaminated from the bottom surface of CFRP as detailed in **c**

interrupted before manually pulling the mandrel) exhibiting a quality issue where the brittle delamination occurred on the bottom surface of the CFRP workpiece, as detailed in Fig. 3c. A similar quality issue was also observed in the FSBR joining of cast magnesium (Mg) alloy sheets, which exhibit poor ductility at room temperature [14]. Such quality issues were not observed in FSBR of aluminum alloy sheets because of the relatively greater ductility and larger thermal conductivity of aluminum as compared to CFRP and Mg alloys (http://www.engineeringtoolbox.com/thermal-conductivity-d_429.html).

When the top CFRP was replaced with the AA6111 (combination II), the process window was broadened. In addition to the conditions shown in Table 2 for CFRP-CFRP joining, AA6111-CFRP joints can be joined at ω=3,000 rpm, v=60 mm min^{-1} and ω=6,000, v=120 mm min^{-1}. This expanded process window can be explained by the greater heat generation during the frictional penetration of the AA6111 sheet. Since the AA6111 possesses a greater strength and higher melting temperature (see Table 1) than the Nylon matrix of the CFRP, more energy input was required and, thus, more heat generation in the frictional penetration of the AA6111 than the CFRP sheet. A detailed comparison of energy input during FSBR of AA6111 and CFRP sheets is made in Section 4. When the heat generated in the AA6111 is transferred to the CFRP bottom sheet, the CFRP sheet softens which facilitates rivet penetration. Another factor is the fact that the mandrel tip temperature is greater after penetrating an AA6111 upper sheet vs. a CFRP upper sheet. Thus, as the mandrel penetrates into the CFRP bottom sheet, a mandrel tip "preheated" by the aluminum top sheet to a higher temperature would penetrate the CFRP with less effort than a cooler mandrel tip which passed through a CFRP top sheet. Outside of the process window, the AA6111-CFRP joints exhibited the same quality issues as presented in Fig. 3a.

From this process window investigation, it can be seen that successful CFRP and AA6111 joints can be fabricated using FSBR within a few seconds. When the stack-up consists of the CFRP and AA6111 on the top and bottom, respectively (combination III), the process window contains a significantly wider spindle speed and feed rate range than for combination I and II joints. The broader process window may be attributed to the fact that the AA6111 bottom workpiece provided a firm support to the CFRP workpiece. When operating FSBR outside of the process window, the support from the AA6111 sheet is insufficient leading the CFRP top workpiece to crack as shown in Fig. 3b.

4 Penetration force and torque during joining

The penetration force and torque histories during FSBR were recorded because they can be used to understand the differences in the process windows for different material combinations. The penetration force and torque are first analyzed with respect to material stack-up sequence, followed by analysis with respect to the process parameters: feed rate and spindle speed.

Figure 4 shows the F_Z vs. Z and M_Z vs. Z curves of the AA6111-CFRP, CFRP-CFRP, and CFRP-AA6111 joints at ω=9,000 rpm and v=120 mm min^{-1}. It is noted here that Z was derived from the feed rate (v) and time (t) and not from a direct real-time measurement, namely, $z=v\cdot t$. It is observed that the peak force (F_{Z_P}) for a rivet penetrating the AA6111 top sheet (AA6111-CFRP joint) is two times that for the CFRP top sheet (CFRP-CFRP joint), and the torque in the former is

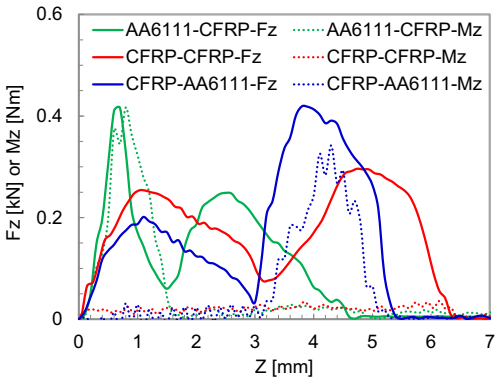

Fig. 4 Force (F_Z vs. Z) and torque (M_Z vs. Z) histories during the joining of a 0.9 mm AA6111-3.0 mm CFRP joint, a CFRP-CFRP joint, and a CFRP-AA6111 joint at ω=9,000 rpm, v=120 mm min^{-1}

correspondingly larger than that in the latter. It is also observed in the CFRP-AA6111 joint that the F_{Z_P} corresponding to the rivet penetrating the AA6111 bottom sheet is comparable to that for the rivet penetrating the AA6111 top sheet (AA6111-CFRP joint); however, the peak torque was significantly reduced. It can be concluded that the penetration force and torque are highly dependent on the stacking sequence of aluminum and CFRP sheets.

The energy consumed during the penetration of AA6111 (E_{6111}) or CFRP (E_{CFRP}) can be calculated by Eq. (1):

$$E_{6111} \text{ or } E_{CFRP} = \int_0^T (F_Z \cdot v)\mathrm{d}t + \int_0^T (2\pi \cdot M_Z \cdot \omega)\mathrm{d}t \qquad (1)$$

where t is time and T is the total time for the rivet penetration through the AA6111 (T_{6111}) or the CFRP workpiece (T_{CFRP}). For the case shown in Fig. 4, T_{6111} was 0.8 s and T_{CFRP} was 1.5 s for the AA6111 top sheet (AA6111-CFRP joint) and the CFRP top sheet (of the CFRP-CFRP joint), respectively. Here, it is noted that due to the formation of a drawing lip on the bottom side of the AA6111 top sheet (as detailed by Min et al. [13]), the rivet requires more than 0.9 mm travel (the thickness of the aluminum sheet) and more than the corresponding 0.45 s to fully penetrate the AA6111 sheet. Consequently, the first trough in the F_Z (or M_Z) vs. Z curve for the AA6111-CFRP joint, refer to Fig. 4, corresponds to complete penetration of the rivet through the AA6111 top sheet and occurred at approximately Z=1.6 mm. In the CFRP-CFRP or CFRP-AA6111 joint, the first trough in the F_Z vs. Z curve appeared at Z~3.0 mm, which corresponds to the thickness of the CFRP top sheet and is consistent with the observation that no drawing lip was formed on the bottom side of the CFRP top sheet. Furthermore, the energy was E_{6111}=150 J for the rivet to travel through the AA6111 top sheet (AA6111-CFRP joint) and E_{CFRP}=22 J for the rivet to travel through the CFRP top sheet (CFRP-CFRP joint). Therefore, when joining the AA6111-CFRP joint, more heat was generated and transferred to the mandrel tip and to the bottom CFRP workpiece when the rivet penetrated through the AA6111 sheet than during the joining of the CFRP-CFRP joint. Consequently, the bottom CFRP in the AA6111-CFRP joint was warmer and more ductile than that in the CFRP-CFRP joint, and the rivet tip had a higher temperature after it penetrated through an AA6111 than a CFRP workpiece; hence, the AA6111-CFRP joint showed a wider process window than the CFRP-CFRP joint as reported in Tables 2 and 3.

The effects of FSBR process parameters on the force and torque when the rivet penetrates an AA6111 sheet were investigated in detail by Min et al. [13]. The following will focus on the effects of spindle speed and feed rate on the force and torque during the frictional penetration of a CFRP workpiece. Since the CFRP-AA6111 joints showed the widest process window and the CFRP workpiece was the top sheet, namely, there was no penetration of the AA6111 prior to the frictional penetration process in the CFRP, the analyses on the force and torque in the CFRP were focused on 0≤Z≤3.0 mm in the CFRP-AA6111 joints.

Table 3 Process window of the AA6111-CFRP joints by FSBR

Spindle speed [rpm]	Feed rate [mm min^{-1}]				
	60	120	270	420	600
3,000	√	QI	QI	–	–
6,000	√	√	QI	QI	–
9,000	√	√	QI	QI	–

√ sound joint, *QI* quality issue, – not tested

Figure 5a is a plot of F_Z vs. Z curves during FSBR of CFRP-AA6111 (combination III) under different spindle speed and feed rate settings. It is worth noting the force history when brittle delamination occurs in the bottom side of the CFRP workpiece. For an example joint (ω=9,000 rpm and v=600 mm min^{-1}) exhibiting the quality issue, shown in Fig. 3b, c, an early sharp drop of F_Z occurs at approximately Z=2.0 mm as indicated by the arrow in Fig. 5a. This is attributed to the delamination of the chip (see Fig. 3a) on the bottom surface of the CFRP top sheet which occurs because of the high penetration force (~1.8 kN). With the support of the AA6111 workpiece that was placed beneath the CFRP, a residual F_Z was required which stabilized at approximately 0.8 kN before the rivet reached the upper surface of the AA6111 bottom sheet (Z=3.0 mm). As shown in Fig. 5b, early abrupt drops in the F_Z vs. $_Z$ curves were also observed in joints exhibiting quality issues from the other two material combinations. This is related to the brittle delamination occurring on the bottom surface of the CFRP bottom sheet. Without any support below the bottom surface of the CFRP bottom sheet, the CFRP-CFRP joint and the AA6111-CFRP joints could not be produced without quality issues under the same process settings that produced good CFRP-AA6111 joints. The critical forces that caused delamination in the CFRP for both the CFRP-CFRP and AA6111-CFRP joints were also substantially lower than those in the CFRP-AA6111 joints because of the greater heat generation when the rivet penetrated the AA6111 top sheet which preheats the CFRP bottom sheet reducing the torque required to penetrate the CFRP bottom sheet compared to the CFRP-CFRP configuration.

For the joints without quality issues (refer to Table 4), the F_Z curves exhibit an initial increase, then plateau, followed by a decrease with penetration depth with no clearly defined peaks in the frictional penetration of the CFRP (Fig. 5a). These relatively stable curves for FSBR of CFRP are different from the curves during FSBR of aluminum alloys sheets,

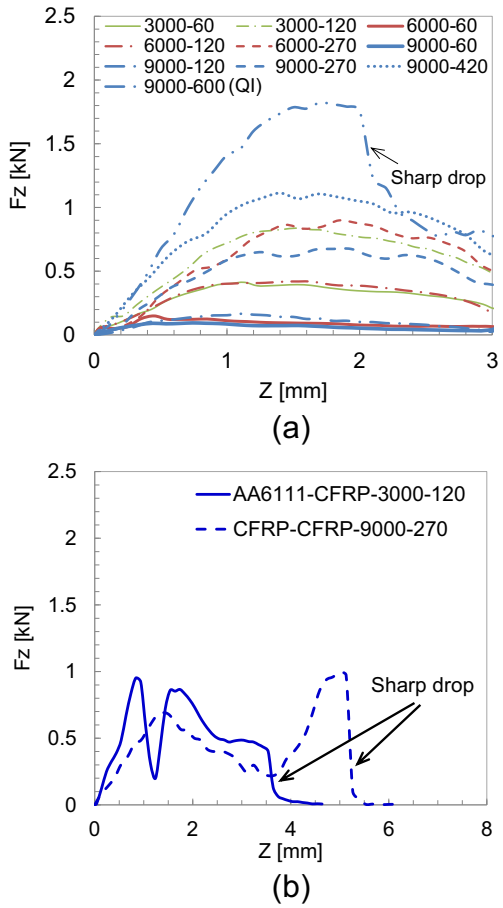

Fig. 5 Force histories (F_Z vs. Z) within the CFRP sheet during FSBR. **a** The CFRP-AA6111 joints at various spindle speeds and feed rates. **b** The AA6111-CFRP joint (ω=3,000 rpm and v=120 mm min^{-1}) and CFRP-CFRP joint (ω=9,000 rpm and v=270 mm min^{-1}) with the quality issue

where the force steadily increases with penetration depth to a peak value before sharply decreasing to zero as the rivet fully penetrates the stack-up. This difference can again be traced back to the differences in thermal conductivity and ductility between aluminum alloy and CFRP. Under all circumstances, M_Z fluctuated within a range of 0 to 0.1 Nm, which was too low to be detectable with the torque sensor, and showed no clear dependence on the process parameters; hence, M_Z vs. Z curves are not reported here for the penetration through CFRP.

In summary, both the stack-up sequence and process parameters exhibited an impact on the force and torque during FSBR of CFRP to CFRP and CFRP to aluminum alloy. Specifically, placing Al alloy on the top can preheat the mandrel tip before the frictional penetration of the bottom CFRP; in the other case, the bottom Al alloy provides support for the top CFRP. In both ways, the Al alloy helps to suppress the occurrence of, though not eliminate, quality issues in the dissimilar joints.

Table 4 Process window of the CFRP-AA6111 joints by FSBR

Spindle speed [rpm]	Feed rate [mm min^{-1}]				
	60	120	270	420	600
3,000	√	√	QI	QI	–
6,000	√	√	√	QI	QI
9,000	√	√	√	√	QI

√ sound joint, *QI* quality issue, – not tested

5 Tensile test results of the FSBR lap joints

As shown above, the material stack-up, spindle speed, and feed rate affect the FSBR process. It is also interesting to study how these factors affect the mechanical performance of the FSBR lap joints and their fracture mode.

Figure 6a, b shows a fractured CFRP-CFRP lap shear joint fabricated at ω=9,000 rpm and v=60 mm min^{-1} and tensile load-displacement curves of the CFRP-CFRP joints fabricated at various process parameters, respectively. Each curve is from a representative tensile test for each joint condition (the same below). All of the CFRP-CFRP joints exhibited fractures in the bottom sheet (refer to Fig. 6). This preference of fracture in the CFRP bottom sheet can be explained by the fact that the large diameter of the shank head can distribute the load over a larger area in the top sheet than what the rivet tail can in the bottom sheet. It is also believed that because of the relative brittleness of the CFRP, the CFRP bottom sheet incurs damage when the shank is upset during tail forming as illustrated in Fig. 1d, e. As shown in Fig. 6b, for the joints without quality issues, the spindle speed and feed rate exhibited little effect upon either the maximum tensile load, approximately 4.2 kN, or the maximum displacement, approximately 3.8 mm. The CFRP-CFRP joint fabricated at 6,000 rpm and 120 mm min^{-1} exhibiting the quality issue sustained a lower maximum load, approximately 3.8 kN that is ~10 % lower than that of the sound joints, but similar maximum displacement.

Figure 7a shows a fractured AA6111-CFRP lap shear joint (fracture in the CFRP bottom sheet) fabricated using the same FSBR parameters as those used to fabricate the samples in Fig. 6a. Nevertheless, the upper AA6111 workpiece underwent significant bending during tensile loading due to the existence of the torque (M) as indicated by the hollow arrow, and this torque increased with increasing tensile load and bending angle (θ) of the AA6111 workpiece. The existence of the torque (M) and rotation of the rivet led to point loading and a stress concentration at the hole edge of the CFRP bottom sheet. As a result, the maximum tensile loads (~3.4 kN) of the AA6111-CFRP joints in Fig. 7b are lower than those of the CFRP-CFRP joints in Fig. 6b. Additionally, the load-displacement curves of the AA6111-CFRP joints exhibit a plateau, which is believed to be associated with bending of the AA6111 top sheet. As in the case for the

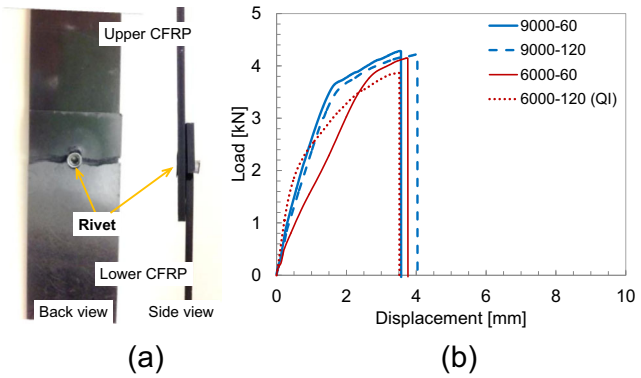

Fig. 6 **a** Photograph of a fractured CFRP-CFRP joint fabricated at ω=9,000 rpm and v=60 mm min^{-1} and **b** load vs. displacement curves of CFRP-CFRP joints at various spindle speeds and feed rates

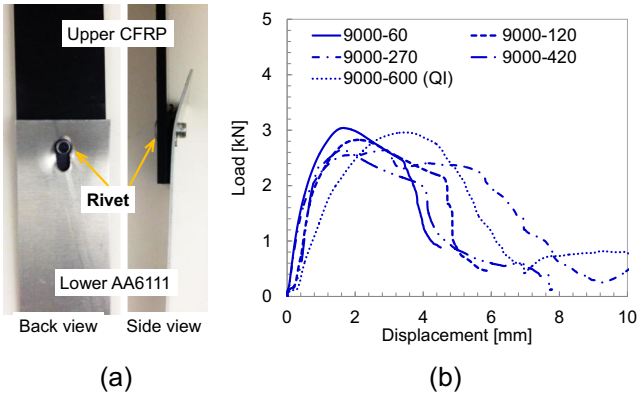

Fig. 8 **a** Photograph of a fractured CFRP-AA6111 joint fabricated at ω=9,000 rpm and v=60 mm min^{-1} and **b** load vs. displacement curves of CFRP-AA6111 joints at various spindle speeds and feed rates

CFRP-CFRP joints, there was no obvious relationship between either spindle speed or feed rate and the maximum tensile load of the AA6111-CFRP joints. The AA6111-CFRP joint with the quality issue fractured at a ~10 % lower maximum tensile load (3.1 kN) and did not show a plateau on the load-displacement curve, since the lower maximum tensile load did not cause substantial bending deformation in the AA6111 workpiece and, consequently, a much smaller maximum displacement (2.2 mm) compared to that of the sound joints (5–6 mm).

Interestingly, the CFRP-AA6111 joints fractured by the rivet slipping out of the AA6111 bottom sheet as shown in Fig. 8a. As observed in the tensile tests, the AA6111 bottom sheet first exhibited a shearing fracture mode followed by the rivets pulling out. The AA6111 bottom sheet underwent more substantial tearing and bending than in the case of the AA6111-CFRP joints during tensile loading. When the bending angle increased to a "threshold" value, the rivet slipped out of the AA6111 workpiece as the rivet tail was no longer able to lock the sheets together. This mode of rivet slipping in the CFRP-AA6111 joints is different from the situation in the AA6111-CFRP joints where the shank head locked the AA6111 workpiece firmly to the CFRP workpiece. Furthermore, it is noted that the AA6111 bottom sheet in the CFRP-AA6111 joints sheared out under tensile loads (~3.1 kN) which were lower than loads (~3.4 kN) carried by the AA6111-CFRP joints; however, in this case, the AA6111 top sheet did not shear out. It is believed that the shank head relieved the stress concentration in the AA6111 sheet in the AA6111-CFRP joints. Finally, it is noted that the quality issue associated with the brittle spalling off the bottom surface of the CFRP sheet did not affect the maximum tensile load of the CFRP-AA6111 joint since the fracture initiated in the AA6111 sheet as shown in Fig. 8a.

In summary, the tensile strength and fracture mode of lap shear FSBR joints is only dependent on the material stack-up and insensitive to process parameters that fall within the process window. The quality issue associated with the brittle spalling off the bottom surface of CFRP only leads to a 10 % reduction in strength in CFRP-CFRP and AA6111-CFRP joints and does not affect the strength of CFRP-AA6111 joints. Based on these observations, the FSBR process is robust in producing consistent joint strength.

6 Concluding remarks

Friction stir blind riveting was successfully applied to join carbon fiber-reinforced polymer composite and aluminum alloy

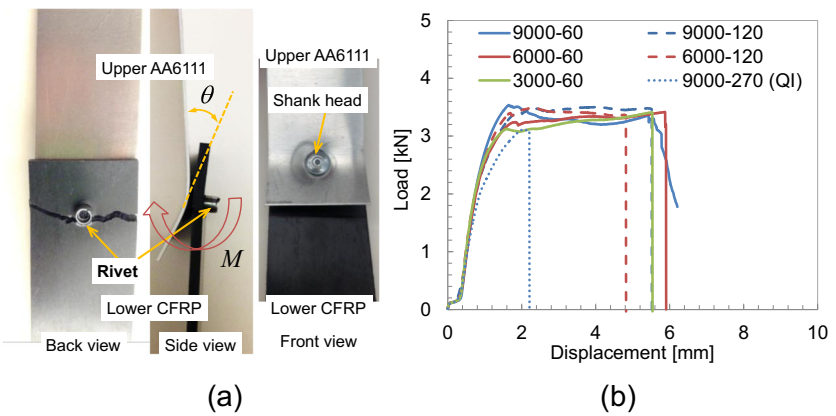

Fig. 7 **a** Photograph of a fractured AA6111-CFRP joint fabricated at ω=9,000 rpm and v=60 mm min^{-1} and **b** load vs. displacement curves of AA6111-CFRP joints at various spindle speeds and feed rates

sheets. Rotating at a high speed, the rivet penetrated through the sheet materials within a few seconds without requiring preexisting holes. The brittleness of the CFRP material was found to be the deterministic factor that limits the size of the process window. In each material combination, a quality issue, i.e., delamination on the backside of the CFRP sheet, was observed at relatively low spindle speeds and higher feed rates.

Because of the striking differences in the mechanical and thermal properties between the aluminum alloy and CFRP sheets, both the FSBR process and the lap shear performance of the dissimilar material joints were greatly affected by the stack-up sequence of the sheets. Among the three combinations studied, the CFRP-CFRP joints exhibited the narrowest process window without quality issue, and the CFRP-AA6111 joints exhibited the widest. In the lap shear tensile tests, the CFRP-CFRP and AA6111-CFRP joints fractured in the CFRP workpiece, and the CFRP-AA6111 joints fractured in the AA6111 workpiece where the AA6111 sheared out before the rivet slipped out of the AA6111 workpiece in the end. Within the process windows, the spindle speed and feed rate did not exhibit any obvious effect on the maximum tensile load of the FSBR joints. Operating slightly outside of the process windows, the quality issue related to brittle delamination of the CFRP sheet caused a 10 % reduction in maximum tensile loads of the CFRP-CFRP and Al-CFRP joints. The same quality issue did not affect the maximum tensile load of the CFRP-Al joint significantly. Based on these observations, the FSBR process is robust in producing consistent joint strength.

Acknowledgments The authors would like to thank Anthony J. Blaszyk and John S. Agapiou for their help in the FSBR tests and David Okonski and Saul Lee for molding the CFRP plaques. The authors are also grateful to BASF for providing the CFRP pellets and Avdel® for providing the rivets. Financial support for this research was provided by the National Science Foundation Civil, Mechanical and Manufacturing Innovation grant no. 1363468 and the project under grant no. 51375346 of the China National Natural Science Foundation.

References

1. He X, Gu F, Ball A (2012) Recent development in finite element analysis of self-piercing riveted joints. Int J Adv Manuf Technol 58: 643–649
2. Antonino V, Vincenzo F, Livan F (2011) Mechanical behaviour and failure modes of metal to composite adhesive joints for nautical applications. Int J Adv Manuf Technol 53:593–600
3. Li C, Liu L (2013) Investigation on weldability of magnesium alloy thin sheet T-joints: arc welding, laser welding, and laser-arc hybrid welding. Int J Adv Manuf Technol 65:27–34
4. Wei S, Li Y, Wang J, Liu K, Zhang P (2014) Microstructure and joining mechanism of Ti/Al dissimilar joint by pulsed gas metal arc welding. Int J Adv Manuf Technol 70:1137–1142
5. Hufenbach W, Dobrzański LA, Gude M, Konieczny J, Czulak A (2007) Optimisation of the rivet joints of the CFRP composite material and aluminium alloy. J Achiev Mater Manuf Eng 20:119–122
6. Casas-Rodriguez JP, Ashcroft IA, Silberschmidt VV (2008) Damage in adhesively bonded CFRP joints: sinusoidal and impact-fatigue. Compos Sci Technol 68:2663–2670
7. Anyfantis KN, Tsouvalis NG (2013) Loading and fracture response of CFRP-to-steel adhesively bonded joints with thick adherents—part II: numerical simulation. Compos Struc 96:858–868
8. Jung KW, Kawahito Y, Takahashi M, Katayama S (2013) Laser direct joining of carbon fiber reinforced plastic to zinc-coated steel. Mater Des 47:179–188
9. Jung KW, Kawahito Y, Katayama S (2011) Laser direct joining of carbon fibre reinforced plastic to stainless steel. Sci Technol Weld Join 16:676–680
10. Lin J, Hua D, Wang PC, Lu Z, Min J (2013) Effect of thermal exposure on the strength of adhesive-bonded low carbon steel. Int J Adhes Adhes 43:70–80
11. Gao D, Ersoy U, Stevenson R, Wang PC (2009) A new one-sided joining process for aluminum alloys: friction stir blind riveting. ASME J Manuf Sci Eng 131:1–12
12. Lathabai S, Tyagi V, Ritchie D, Kearney T, Finnin B (2011) Friction stir blind riveting: a novel joining process for automotive light alloys. SAE Int J Mater Manuf 4:589–601
13. Min J, Li J, Li Y, Carlson BE, Lin J, Wang W (2015) Friction stir blind riveting of aluminum alloy sheets. J Mater Process Technol 215:20–29
14. Min J, Li J, Carlson BE, Li Y, Quinn JF, Lin J, Wang W (2014) Friction stir blind riveting for dissimilar cast Mg AM60 and Al alloy sheets. Proceedings of ASME 2014 Manufacturing Science and Engineering Conference, June 9–13, Detroit, Michigan